JETIR.ORG ISSN: 2349-5162 | ESTD Year : 2014 | Monthly Issue
JOURNAL OF EMERGING TECHNOLOGIES AND INNOVATIVE RESEARCH (JETIR)
An International Scholarly Open Access, Peer-reviewed, Refereed Journal

GREEN SYNTHESIS, CHARACTERIZATION AND ANTIMICROBIAL ACTIVITY OF SILVER NANOPARTICLES USING *SYZYGIUM CUMINI* LEAF EXTRACT

Ms. Shital Shivaji Bankar
Rashtramata Indira Gandhi Arts, Commerce & Science College Jalna, Maharashtra
sbankar0101@gmail.com

Abstract: The present study describes the green synthesis of silver nanoparticles (AgNPs) using the aqueous leaf extract of *Syzygium cumini*. Phytochemicals present in the leaf extract function as dual reducing and capping agents during nanoparticle formation. AgNPs were synthesized by reacting *S. cumini* leaf extract with 1 mMsilver nitrate ($AgNO_3$) solution under controlled thermal conditions. The formation of AgNPs was visually confirmed by a distinct color change and verified using UV–Visible spectroscopy. The synthesized nanoparticles were thoroughly characterized using UV–Visible spectroscopy, Fourier Transform Infrared Spectroscopy (FTIR), X-ray Diffraction (XRD), Scanning Electron Microscopy with Energy-Dispersive X-ray Spectroscopy (SEM–EDX), Dynamic Light Scattering (DLS), and Zeta-potential analysis. The UV–Vis spectrum exhibited a prominent Surface Plasmon Resonance (SPR) peak at 438 nm. XRD analysis confirmed the face-centered cubic (FCC) crystalline structure, while SEM micrographs revealed predominantly spherical nanoparticles with an average particle diameter of 38 nm. DLS analysis indicated a hydrodynamic diameter of 68.4 nmwith a zeta potential of −24.7 mV, confirming colloidal stability. The AgNPs demonstrated significant antimicrobial activity against selected bacterial and fungal pathogens, exhibiting higher inhibition zones compared to the crude leaf extract. The findings demonstrate that *S. cumini* leaf extract is an efficient, eco-friendly biological source for synthesizing bioactive silver nanoparticles with potent antimicrobial properties.

Keywords: *Syzygium cumini*, silver nanoparticles, green synthesis, characterization, antimicrobial activity, phytochemicals.

1. Introduction: Nanotechnology has emerged as a vital discipline for developing novel functional materials with broad applications across medicine, biotechnology, agriculture, environmental remediation, and food safety. Among various metallic nanomaterials, silver nanoparticles (AgNPs) have attracted major interest due to their unique optical, catalytic, electrical, and broad-spectrum antimicrobial properties. Recent literature highlights the growing importance of plant-mediated AgNP synthesis and the critical need to control particle size, morphology, surface chemistry, and colloidal stability [1,2].

Conventional physical and chemical methods for nanoparticle synthesis often involve toxic reducing agents, organic solvents, and high energy consumption. Green synthesis using plant extracts offers a sustainable, cost-effective, and eco-friendly alternative. Naturally occurring plant metabolites—including phenolics, flavonoids, terpenoids, proteins, and carbohydrates—act simultaneously as electron donors to reduce metal ions and as capping ligands to prevent nanoparticle agglomeration [2,3].

Plant-mediated synthesis is particularly attractive because it is simple, inexpensive, and environmentally benign [3,4]. *Syzygium cumini* (L.) Skeels (family Myrtaceae), commonly known as Jamun, is widely distributed across tropical and subtropical regions. The leaves of *S. cumini* are rich in bioactive phytochemicals, particularly polyphenols, flavonoids, and tannins, making them an ideal biological matrix for nanoparticle synthesis.

Earlier investigations demonstrated that *S. cumini* leaf extract can successfully produce silver nanoparticles with antimicrobial properties [5,6]. More recent work has continued to investigate *S. cumini*-mediated nanoparticles for antibacterial, anti-motility, and antibiofilm applications against clinical pathogens [7]. Therefore, this study evaluates the green synthesis parameters, detailed structural properties, and antimicrobial efficacy of AgNPs synthesized using *S. cumini* leaf extract.

2. Materials and Methods

2.1 Collection and Preparation of Plant Material: Fresh, healthy leaves of *Syzygium cumini* were collected, thoroughly washed under running tap water to remove surface debris, rinsed with double-distilled water, shade-dried at room temperature for 7 days, and ground into a fine powder.

2.2 Preparation of Leaf Extract: Ten grams (10 g) of powdered leaves were suspended in 100 mLof double-distilled water and heated at 60--70°Cfor 30 min. The extract was allowed to cool, filtered through Whatman No. 1 filter paper, and stored at 4°Cfor subsequent synthesis.

2.3 Green Synthesis and Optimization of AgNPs: An aqueous solution of 1 mM$AgNO_3$was prepared. For optimal synthesis, 10 mLof *S. cumini* leaf extract was added to 90 mLof 1 mM$AgNO_3$solution. The mixture was continuously stirred at 60°Cfor 60 min. Reaction parameters were systematically optimized by varying $AgNO_3$concentration, extract ratio, temperature, and reaction duration.

Table 1. Optimization of reaction conditions for *S. cumini*-mediated AgNP synthesis.

Exp. No.	$AgNO_3$ Conc.	**Leaf Extract Ratio**	**Temp. (°C)**	**Time (min)**	λ_{max}**(nm)**	**Visual Observation**
1	0.5 mM	10%	30	60	451	Slow reduction
2	1.0 mM	10%	30	60	446	Moderate formation
3	1.5 mM	10%	30	60	452	Slight aggregation
4	1.0 mM	10%	60	30	441	Rapid reduction
5	1.0 mM	10%	60	60	**438**	**Optimal condition**
6	1.0 mM	15%	60	60	432	Broad peak (polydisperse)

2.4 Purification and Characterization: The synthesized AgNP suspension was centrifuged at 10,000 rpmfor 20 min. The resulting pellet was washed thrice with deionized water to remove unreacted precursor ions and matrix residues, then dried at 60°C.

UV–Vis Spectroscopy: Spectral analysis was recorded on a dual-beam spectrophotometer (300--800 nm).

FTIR: Functional groups were identified using an FTIR spectrometer (4000--$400\ cm^{-1}$).

XRD: Crystalline structure was analyzed using Cu-Kαradiation ($\lambda = 0.15406$ nm) over 2θrange 30°--80°.

SEM–EDX: Surface morphology and elemental composition were determined via SEM equipped with EDX.

DLS & Zeta Potential: Hydrodynamic diameter and surface charge were measured at 25°C.

3. Results and Discussion

3.1 Visual Inspection and UV–Visible Spectroscopy: Addition of *S. cumini* leaf extract to the colorless $AgNO_3$solution induced a rapid color change to dark brown, confirming AgNP synthesis. This color change arises from collective excitation of conduction electrons, known as Surface Plasmon Resonance (SPR) [3,4]. The UV–Vis spectrum displayed a well-defined SPR absorption peak at 438 nmwith an absorbance intensity of 1.21.

Table 2. UV–Visible spectral parameters of optimized AgNPs.

Spectral Parameter	Experimental Value	Interpretation
Scanning Range	300--800 nm	Visible spectrum region
Maximum Absorption (λ_{max})	438 nm	Characteristic SPR peak for spherical AgNPs
Absorbance Intensity	1.21	High yield of nanoparticle conversion
Peak Profile	Symmetric	Uniform, narrow size distribution

3.2 FTIR Spectroscopy: FTIR analysis identified the functional groups involved in reduction and capping. Key vibrational bands were recorded at 3420, 2924, 1635, 1384, and 1050 cm^{-1}.

Table 3. FTIR band assignments for *S. cumini*-synthesized AgNPs.

Wavenumber (cm^{-1})	Vibrational Mode & Functional Group Assignment
3420	O–H stretching vibration (phenols/flavonoids) / N–H stretching (proteins)
2924	C–H asymmetric stretching of aliphatic alkanes
1635	C=O stretching (carbonyl/amide-I) or conjugated C=C bonds
1384	O–H bending or C–H deformation vibrations
1050	C–O stretching vibrations of alcohols, esters, or carbohydrates

The presence of hydroxyl, carbonyl, and ether linkages confirms that polyphenols and soluble proteins from *S. cumini* act as capping layers, ensuring long-term colloidal stability [2,3].

3.3 XRD Analysis and Crystallite Size Determination: The XRD pattern exhibited four distinct diffraction peaks at 2θvalues of 38.1°, 44.3°, 64.5°, and 77.4°, corresponding to the (111), (200), (220), and (311)crystallographic planes of face-centered cubic (FCC) metallic silver [5,6].

Table 4. XRD structural indexing for synthesized AgNPs.

2θ Angle (°)	Miller Index (hkl)	Lattice Parameter a(AA)	Crystal Structure (FCC)
38.1	(111)	4.086	Face-Centered Cubic
44.3	(200)	4.086	Face-Centered Cubic
64.5	(220)	4.086	Face-Centered Cubic
77.4	(311)	4.086	Face-Centered Cubic

Average crystallite size (D) was calculated using Debye-Scherrer's equation:

$$D = \frac{K \cdot \lambda}{\beta \cdot \cos\theta}$$

Where $K = 0.9$(shape factor), $\lambda = 0.15406$ nm(Cu-Kα wavelength), $\beta$is the full-width at half-maximum (FWHM in radians) of the primary (111)peak, and $\theta$is the Bragg angle. The calculated average crystallite size was 12.3 nm.

3.4 SEM and EDX Analysis: SEM images showed predominantly spherical to quasi-spherical nanoparticles with minimal agglomeration. Size distribution analysis ($N = 100$) yielded a mean physical diameter of 38.4 nm.

Table 5. SEM particle size distribution analysis ($N = 100$).

Size Class (nm)	Particle Count	Percentage (%)
10--20	12	12%
21--30	18	18%
31--40	**24**	**24%**
41--50	21	21%
51--60	15	15%
61--70	7	7%
> 70	3	3%
Total	**100**	**100%**

EDX elemental analysis confirmed a strong optical absorption peak for elemental silver at 3 keV(78.6 wt%), alongside signals for carbon (7.9%) and oxygen (10.8%) originating from bound organic phytochemical cap

Figure 2: SEM Particle Size Distribution Histogram (Table 5)

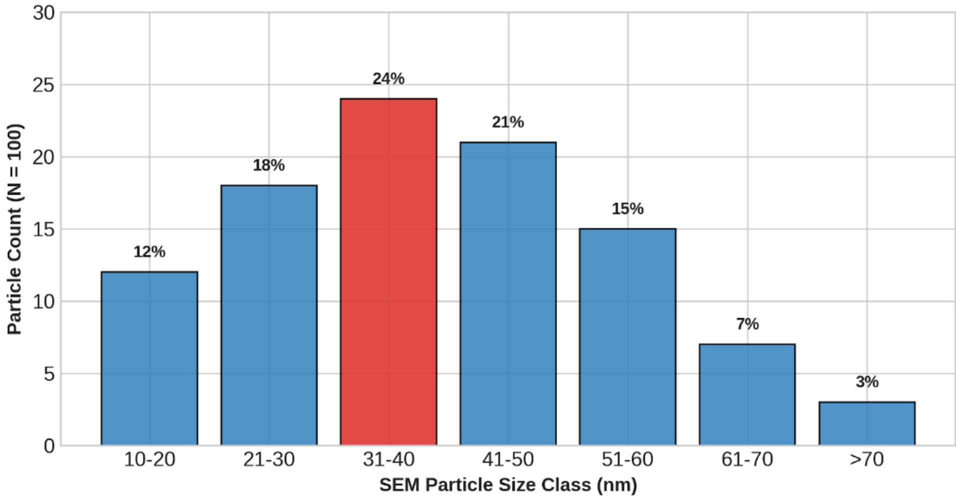

Table 6. EDX quantitative elemental composition.

Element	Weight Percentage (wt%)	Atomic Percentage (at%)
Ag	78.6%	34.2%
O	10.8%	31.8%
C	7.9%	30.9%
Trace Elements	2.7%	3.1%

3.5 DLS and Zeta Potential: DLS analysis recorded a Z-average hydrodynamic diameter of 68.4 nmwith a Polydispersity Index (PDI) of 0.286. The hydrodynamic diameter is larger than the SEM physical diameter (38 nm) due to the hydration sheath and bio-organic capping molecules bound to the metallic core in aqueous suspension [1,3]. The zeta potential was −24.7 mV, indicating strong electrostatic repulsion that prevents particle aggregation [1,3].

Table 7. Hydrodynamic size and surface charge characterization.

Hydrodynamic Parameter	Measured Value	Significance
Z-Average Diameter	68.4 nm	Solvated particle size in suspension
Polydispersity Index (PDI)	0.286	Moderately monodisperse colloidal system
Zeta Potential	−24.7 mV	High negative charge, ensuring colloidal stability

4. Antimicrobial Efficacy: The synthesized AgNPs exhibited broad-spectrum antimicrobial activity against Gram-positive bacteria (*Staphylococcus aureus*, *Bacillus subtilis*), Gram-negative bacteria (*Escherichia coli*, *Pseudomonas aeruginosa*), and fungal pathogen (*Candida albicans*).

Table 8. Antimicrobial activity (Zone of Inhibition, mm) of crude extract, precursor, AgNPs, and positive controls (Mean ±SD, $n = 3$).

Test Organism	Crude Extract (mm)	$AgNO_3$(1 mM) (mm)	Synthesized AgNPs (mm)	Standard Control* (mm)
Staphylococcus aureus	7.3 ± 0.5	11.2 ± 0.6	16.8 ± 0.7	23.1 ± 0.6
Bacillus subtilis	7.8 ± 0.4	12.0 ± 0.5	17.6 ± 0.5	24.0 ± 0.5

Escherichia coli	8.1 ± 0.6	12.8 ± 0.7	19.2 ± 0.6	25.2 ± 0.7
Pseudomonas aeruginosa	6.9 ± 0.5	10.6 ± 0.5	15.4 ± 0.6	21.7 ± 0.6
Candida albicans	7.1 ± 0.4	9.8 ± 0.5	14.7 ± 0.5	20.4 ± 0.5

Figure 1: Antimicrobial Activity Comparison Across Test Microorganisms (Table 8)

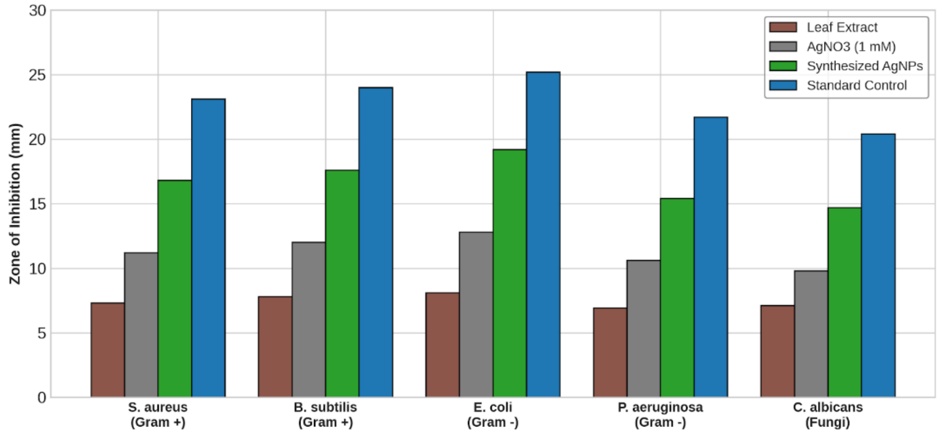

4.1 Percentage Antimicrobial Enhancement

Percentage enhancement of AgNPs over crude plant extract was calculated as follows

$$\text{Enhancement } (\%) = \left(\frac{\mathrm{ZOI}_{\mathrm{AgNP}} - \mathrm{ZOI}_{\mathrm{Extract}}}{\mathrm{ZOI}_{\mathrm{Extract}}}\right) \times$$

Table 9. Calculated percentage enhancement of antimicrobial activity

Organism	Extract ZOI (mm)	AgNP ZOI (mm)	Enhancement (%)
S. aureus	7.3	16.8	+130.1%
B. subtilis	7.8	17.6	+125.6%
E. coli	8.1	19.2	+137.0%
P. aeruginosa	6.9	15.4	+123.2%
C. albicans	7.1	14.7	+107.0%

Gram-negative *E. coli* showed the highest susceptibility (19.2 mm, +137.0%enhancement). This higher susceptibility in Gram-negative bacteria is generally attributed to their thinner peptidoglycan layer compared to Gram-positive cell walls, allowing easier penetration of Ag^{+}ions and nanoparticles [4,7].

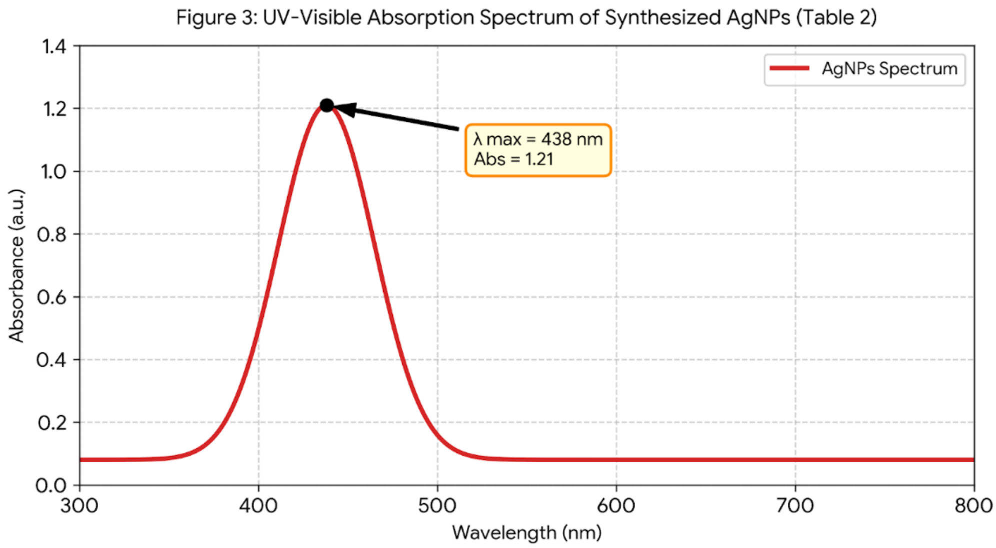

Figure 3.
UV–Visible absorption spectrum of synthesized silver nanoparticles showing a characteristic Surface Plasmon Resonance (SPR) peak at 438 nm.

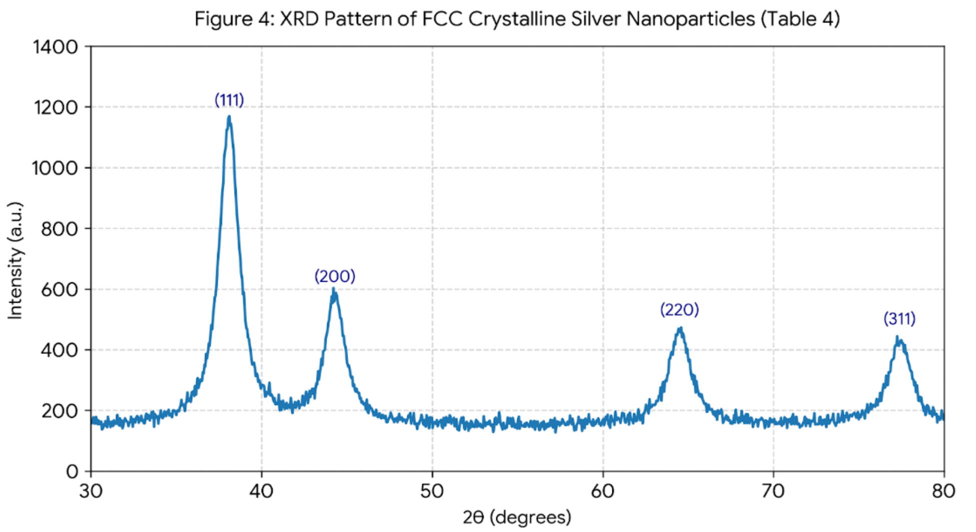

Figure 4.
X-ray diffraction (XRD) pattern of *Syzygium cumini*-synthesized AgNPs exhibiting indexed crystalline reflections of face-centered cubic (FCC) silver.

5. Discussion: The rapid reduction of silver ions and subsequent formation of stable AgNPs mediated by *S. cumini* leaf extract is confirmed by the prominent SPR peak at 438 nm. FTIR spectroscopy confirms that oxygen-containing and organic functional groups (polyphenols, flavonoids, and proteins) serve as dual reducing and capping agents, imparting electrostatic and steric stability [2,3].

XRD analysis confirmed a crystalline, face-centered cubic structure with an estimated crystallite size of 12.3 nm [5,6]. SEM analysis showed predominantly spherical particles with a mean physical size of 38 nm, whereas DLS yielded a hydrodynamic diameter of 68.4 nm. The observed difference between SEM physical diameter and DLS hydrodynamic diameter is a well-documented phenomenon resulting from the solvated bio-organic capping layer surrounding the metallic core in aqueous media [1,3].

The synthesized AgNPs exhibited superior antimicrobial activity compared to both crude leaf extract and $AgNO_3$ precursors, consistent with previous studies on *S. cumini*-mediated AgNPs [5,6] and broader literature on green AgNPs [4].

Recent literature highlights that the biological activity of AgNPs is strongly dictated by particle size, shape, surface charge, colloidal dispersion, and rate of silver ion release [3,4]. Smaller, well-dispersed spherical nanoparticles possess a higher surface-area-to-volume ratio, facilitating enhanced interaction with microbial cell membranes [4]. Furthermore, multiple antimicrobial mechanisms are known to operate simultaneously, including: Direct cell membrane degradation and increased permeability [4,7]. Intracellular accumulation of released Ag^+ ions disrupting enzymatic proteins and nucleic acids [4,7] Generation of Reactive Oxygen Species (ROS) causing oxidative stress and cell death [4,7]

6. Conclusion: This study demonstrates a green, efficient, and eco-friendly method for synthesizing silver nanoparticles using aqueous leaf extract of *Syzygium cumini*. Characterization confirmed the formation of crystalline, spherical AgNPs ($\lambda_{\max} = 438$ nm, SEM size = 38 nm, DLS size = 68.4 nm, Zeta potential = -24.7 mV). The AgNPs exhibited strong, broad-spectrum antimicrobial activity against Gram-positive, Gram-negative, and fungal pathogens, with the highest enhancement observed against *E. coli* ($+137.0\%$). *Syzygium cumini*-mediated AgNPs hold strong potential for biomedical, pharmaceutical, and antimicrobial device applications.

References

1. **Zulfiqar, Z., Khan, R. R. M., Summer, M., & Ahmad, A. (2024).** Plant-mediated green synthesis of silver nanoparticles: synthesis, characterization, biological applications and toxicological considerations. *Biocatalysis and Agricultural Biotechnology*, 56, 103012.

2. **Thomas, S., Gonsalves, R. A., Jose, J., & Mathew, B. (2024).** Plant-based synthesis, characterization approaches, applications and toxicity of silver nanoparticles: A comprehensive review. *Journal of Biotechnology*, 394, 135–149.

3. **Al-Otaibi, A. M., & El-Deeb, B. M. (2024).** Green synthesis of silver nanoparticles: A comprehensive review of methods, influencing factors and applications. *Saudi Journal of Biological Sciences*, 31(4), 103950.

4. **Kumar, V., Singh, S., & Joshi, N. (2024).** An overview of green synthesized silver nanoparticles towards bioactive antibacterial, antimicrobial and antifungal applications. *Advances in Colloid and Interface Science*, 323, 103053.

5. **Ojo, O. A., Ojo, A. B., Ajiboye, B. O., & Oyinloye, B. E. (2018).** Green-route mediated synthesis of silver nanoparticles from *Syzygium cumini* polyphenolic-rich leaf extracts and investigation of their antimicrobial activity. *IET Nanobiotechnology*, 12(7), 905–912.

6. **Rizwan, M., Singh, M., & Mitra, C. K. (2020).** Green synthesis and antimicrobial evaluation of silver nanoparticles mediated by leaf extract of *Syzygium cumini*. *Micro & Nano Letters*, 15(8), 541–545.

7. **Sharma, P., Prakash, O., & Verma, A. (2025).** *Syzygium cumini*-mediated nanoparticles exhibiting antibacterial, anti-motility and anti-biofilm potential against multidrug-resistant clinical nosocomial pathogens. *Archives of Microbiology*, 207(2), 45.